Inorganic Chemistry

Article

pubs.acs.org/IC

Step-by-Step Strategy from Achiral Precursors to Polyoxometalates-Based Chiral Organic–Inorganic Hybrids

Jiangwei Zhang,[†] Jianhui Luo,*[,‡] Pingmei Wang,[‡] Bin Ding,[‡] Yichao Huang,[†] Zhenlin Zhao,[†] Jin Zhang,*[,†] and Yongge Wei*[,†]

[†]Department of Chemistry, Tsinghua University, Beijing 100084, P. R. China

[‡]The Research Institute of Petroleum Exploration & Development (RIPED), and the Key Laboratory of Nano Chemistry (KLNC), PetroChina, Beijing 100083, P. R. China

Supporting Information

ABSTRACT: Using two types of triol ligands, several novel asymmetrically triol-functionalized Anderson organic hybrids have been efficiently synthesized in high purity and good yields via a convenient two-step esterification reaction. These organic–inorganic hybrids are chiral and can be spontaneously resolved with suitable solvents. Their molecular and crystal structures have been confirmed by single-crystal X-ray diffraction studies. Stable solid-state chirality of the corresponding enantiopure crystals has also been confirmed definitively by CD spectra. Interestingly, these organic–inorganic hybrids possess a layer-by-layer structure, forming solvent-accessible nanoscale chiral channels via a 1D infinite helical chain substructure. TGA measurements indicated that the species of the central heteroatoms significantly effects the stability of these compounds.

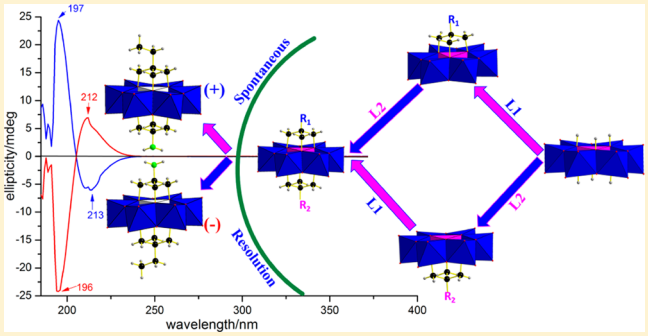

INTRODUCTION

Chirality has become an increasingly vital concern in many fields, ranging from biochemistry to catalysis and pharmaceuticals.[1−3] Applying the materials used in chiral asymmetric catalysis serves as a promising strategy for addressing challenging issues, including energy shortage, environmental pollution, and others, facing modern society.[4] Polyoxometalates (POMs) are a unique family of inorganic oxide clusters that consist of early transition metal ions such as Mo, W, V, and others having structural versatility and being used a wide range applications.[5] In particular, the oxidative catalysis property of POMs has been prominently featured in the field of catalysis in both scientific investigations and industrial projects.[6] Hence, several excellent, pioneering lines of research have been conducted by Hill,[7] Kortz,[8] Cronin,[9] Wang,[10] Hasenknopf,[11] Wei,[12] and other groups;[13] they attempted to combine chirality with the catalytic property of POMs by breaking the symmetry elements in POM clusters. However, the synthesis of stable POM-based chiral materials is an important but challenging task because classic POMs usually possess mirror symmetry, center symmetry, or both. In many cases, even when the symmetry elements have been removed, enantiopure materials still cannot be obtained due to rapid racemization, and stable chirality does not emerge.

Meanwhile, the applications in which POMs can be used can be greatly enriched by anchoring organic moieties on their surfaces. These organic moieties, which contain well-established reactivity sites and specific steric hindrance, make the design of functional materials more accessible and rational,[14] especially when they serve as structure-directing agents in the design of chiral organic–inorganic hybrid materials. Among these organic moieties, triol ligands have been widely applied to grafting on POMs to generate Lindqvist,[15] Dawson,[16] and Anderson[17] framework-based organic hybrids. As one of the basic structure units, Anderson-type clusters are one of the most flexible and tunable structures among the POMs family. Excellent investigations concerning the synthesis of triol, symmetrical, organic-functionalized Anderson derivatives containing Mn as the central heteroatom have been conducted by Cronin,[18] Hasenknopf,[19] and other groups.[20] They introduced different kinds of functional organic moieties to this system through pre- and postfunctionalization. It is not disputed that both sides of an Anderson cluster can be simultaneously functionalized by triol ligands; thus, the center symmetry element still exists. The process involves POM reconstruction from $[Mo_8O_{26}]^{4-}$ to the organic triol-functionalized Anderson derivatives, $\{[RC(CH_2O)_3]_2MnMo_6O_{18}\}^{3-}$.[21] In 2008, Cronin creatively developed a strategy to synthesize triol asymmetrically functionalized Mn–Anderson hybrids by adding two types of triol ligands simultaneously and isolated the asymmetric products from the mixture containing two symmetric byproducts by monitoring crystallization and sorting the clusters with mass spectrometry.[22] They further developed a chromatographic methodology

Received: October 31, 2014
Published: March 5, 2015

DOI: 10.1021/ic502622k
Inorg. Chem. 2015, 54, 2551−2559

to simplify this isolation.[23] Although such a method to separate the desired asymmetric products is universal, it is still ineffective. Moreover, the generation of two symmetric byproducts is inevitable regardless of how the isolation method was developed or optimized. The yield of asymmetric products is not very high, and the separation is time consuming. The obstacles to exploiting POM-baded asymmetric-funtionalized hybrids should be conquered because such hybrids have shown promise for use in applications in biochemistry such as selective cell adhesion[18a] and generating specific peptide chains containing inorganic amino acids.[18e]

Inspired by pioneering work of Hasenknopf and Cronin,[18,19] we hypothesized that a stepwise modification method may address this problem elegantly and make it easy to obtain desired asymmetrical POM-based organic hybrids effectively. This approach would involve first modifying one side of the Anderson cluster using one kind of triol ligand[24] and then the other side by another type of triol ligand. In this article, we will report a series of novel asymmetrically triol-funtionalized Anderson cluster hybrids synthesized by this stepwise modification strategy. The corresponding Anderson derivatives containing remote amino group are the most challenging but valuable synthons to generate for further postfunctionalization. Moreover, we discovered that such asymmetricially triol-funtionalized derivatives are chiral, although all of the precursors are achiral, which makes this protocol more valuable. Since the central heteroatom in an Anderson cluster can be accessible to more than 70 elements in the periodic table, the strategy presented here is general and will remove a significant obstacle to exploiting POM-based funtionalized hybrids as functional synthons, including the design of novel chiral POMs.

EXPERIMENTAL SECTION

General Methods and Materials. $[CrMo_6O_{18}(OH)_6]^{3-}$, $[MnMo_6O_{18}(OH)_6]^{3-}$, and $[AlMo_6O_{18}(OH)_6]^{3-}$ were synthesized according to modified literature methods.[25] The single-sided triol-functionalized precursors $[TBA]_3[RC(CH_2O)_3MMo_6O_{18}(OH)_3]$ (compound **1**: M = Cr^{3+}, R = NH_2; compound **2**: M = Cr^{3+}, R = C_2H_5; compound **3**: M = Mn^{3+}, R = NH_2; compound **4**: M = Al^{3+}, R = C_2H_5) were synthesized according to our previously published protocol.[24]

All synthesis and manipulations were performed in open air; all other chemicals, including solvents, were commercially available, reagent grade, and used as received without further purification from Adamas-beta. IR spectra were measured using KBr pellets and recorded on a PerkinElmer FT-IR spectrometer. UV−vis spectra were measured in acetonitrile with a UV2100s spectrophotometer. Mass spectra were obtained using an ion trap mass spectrometer (Thermofisher LTQ). Negative mode was chosen for the experiments (capillary voltage, 33 V). The sample solution (in acetonitrile) was infused into the ESI source at a flow rate of 300 $\mu L \cdot min^{-1}$. ^1H and ^{13}C NMR spectra were obtained on a JEOL JNM-ECA400 spectrometer and are reported in ppm. Elemental analyses were performed by Elementar Analysensysteme GmbH (vario EL). The solid- and liquid-state circular dichroism (CD) spectra were measured with an Applied Photophysics Chirascan spectropolarimeter. Thermal gravimetric analysis (TGA) measurements were performed with a Mettler Toledo TGA/SDTA851 in flowing Ar (50.0 mL/min) with a heating rate of 20 K/min.

Synthesis and Crystallization. *Synthesis of $[TBA]_3\{[C_2H_5C(CH_2O)_3]CrMo_6O_{18}[(OCH_2)_3CNH_2]\}$ Compound 5. Method A.* A mixture of compound **2** (1.825 g, 1 mmol) and tris(hydroxymethyl) aminomethane (L1) (0.121 g, 1 mmol) was dissolved in 25 mL of ethanol and then refluxed at 78 °C for 3 h. Then, the reaction solution was filtered to remove the white precipitate, and a pink solution was obtained. Then, the filtrate was poured into ether, resulting in precipitation. After the solution cleared, the liquid supernatant was poured off, and the product was deposited as pink crystals (yield 84% based on Mo).

Method B. The synthesis process is similar to that in Method A. A mixture of compound **1** (1.812 g, 1 mmol) and 1,1,1-Tris-(hydroxymethyl) propane (L2) (0.134 g, 1 mmol) was dissolved in 25 mL of ethanol and then refluxed at 78 °C for 3 h (yield 85% based on Mo). Using both Methods A and B, compound **5** can be obtained.

Crystallization of Compound 5. $[TBA]_6\{[C_2H_5C(CH_2O)_3]$-$CrMo_6O_{18}[(OCH_2)_3CNH_2]\}_2 \cdot 3DMF$. Single crystals suitable for X-ray diffraction were grown from a 65:35 DMF/MeCN mixed solvent by slow evaporation. After crystallization, compound **5** was obtained as a pink crystalline product.

Synthesis of $[TBA]_3\{[C_2H_5C(CH_2O)_3]MnMo_6O_{18}[(OCH_2)_3CNH_2]\}$ Compound 6. The synthesis process is similar to that for synthesis of compound **5** except that a mixture of compound **3** (1.815 g, 1 mmol) and 1,1,1-tris(hydroxymethyl)propane (L2) (0.134 g, 1 mmol) was dissolved in 25 mL of ethanol and then refluxed at 78 °C for 3 h (yield 77% based on Mo).

Crystallization of Compound 6. $[TBA]_6\{[C_2H_5C(CH_2O)_3]$-$MnMo_6O_{18}[(OCH_2)_3CNH_2]\}_2 \cdot 4DMF$. Single crystals suitable for X-ray diffraction were grown from a 65:35 DMF/MeCN mixed solvent by slow evaporation. After crystallization, compound **6** was obtained as an orange crystalline product.

Synthesis of $[TBA]_3\{[C_2H_5C(CH_2O)_3]AlMo_6O_{18}[(OCH_2)_3CNH_2]\}$ Compound 7. The synthesis process is similar to that for the synthesis of compound **5** except that a mixture of compound **4** (1.800 g, 1 mmol) and tris(hydroxymethyl) aminomethane (L1) (0.121 g, 1 mmol) was dissolved in 25 mL of ethanol and then refluxed at 78 °C for 3 h (yield 81% based on Mo).

Crystallization of Compound 7. $[TBA]_6\{[C_2H_5C(CH_2O)_3]$-$AlMo_6O_{18}[(OCH_2)_3CNH_2]\}_2 \cdot 3DMF$. Single crystals suitable for X-ray diffraction were grown from a 65:35 DMF/MeCN mixed solvent by slow evaporation. After crystallization, compound **7** was obtained as a colorless crystalline product.

X-ray Crystallographic Structural Determinations. Suitable single crystals were selected (see Figure S1 in Supporting Information), and data collection was performed at 100, 103, 293, 103, 293, 293, and 293 K for compounds **1**−**7**, respectively, using graphite-monochromated Mo Kα radiation (λ = 0.71073 Å) for compounds **1**−**4** and Cu Kα radiation (λ = 1.54184 Å) for compounds **5**−**7**. Data reduction, cell refinement, and experimental absorption correction were performed with Rigaku RAPID AUTO software (Rigaku, 1998, ver 2.30). Structures were solved by direct methods and refined against F^2 by full-matrix least-squares. All non-hydrogen atoms were refined anisotropically. Hydrogen atoms were generated geometrically. All calculations were carried out by SHELXTL, ver 5.1,[26] and Olex2, ver 1.2.6.[27]

Crystal Data. ***1:*** *$[TBA]_3\{[H_2NC(CH_2O)_3]CrMo_6O_{18}(OH)_3\} \cdot [TBA]Br \cdot 2H_2O$.* $C_{68}H_{159}BrCrMo_6N_5O_{26}$, M_r = 2170.55, monoclinic, space group $P2_1$, a = 16.3140(13), b = 15.3614(6), c = 18.1903(8) Å, $\alpha = \gamma = 90°$, β = 92.867(7)°, V = 4552.9(4) Å^3, Z = 2, T = 101(2) K, 28 285 reflections measured, R_1(final) = 0.0359, wR_2 = 0.0933.

2: *$[TBA]_3\{[H_5C_2C(CH_2O)_3]CrMo_6O_{18}(OH)_3\} \cdot [TBA]Br \cdot NH_4Br$.* $C_{70}H_{162}N_5CrMo_6O_{24}Br_2$, M_r = 2245.43, monoclinic, space group $P2_1/n$, a = 16.5994(3), b = 26.2375(6), c = 22.1200(4) Å, $\alpha = \gamma = 90°$, β = 91.7125(17)°, V = 9629.6(3) Å^3, Z = 2, T = 103(2) K, 42 577 reflections measured, R_1(final) = 0.0489, wR_2 = 0.1086.

3: *$[TBA]_3\{[H_2NC(CH_2O)_3]MnMo_6O_{18}(OH)_3\} \cdot [TBA]Br$.* $C_{68}H_{155}BrMnMo_6N_5O_{24}$, M_r = 2137.46, monoclinic, space group $P2_1$, a = 16.1269(13), b = 15.5347(6), c = 17.9890(8) Å, $\alpha = \gamma = 90°$, β = 93.043(7)°, V = 4500.4(4) Å^3, Z = 2, T = 293(2) K, 29 107 reflections measured, R_1(final) = 0.0375, wR_2 = 0.0821.

4: *$[TBA]_3\{[C_2H_5C(CH_2O)_3]AlMo_6O_{18}(OH)_3\} \cdot [TBA]Br$.* $C_{70}H_{158}AlBrMo_6N_4O_{24}$, M_r = 2122.54, monoclinic, space group $P2_1$, a = 15.9787(3), b = 15.8012(3), c = 18.1275(3) Å, $\alpha = \gamma = 90°$, β= 93.1770(18)°, V = 4569.86(16)Å^3, Z = 2, T = 103(9) K, 36 622 reflections measured, R_1(final) = 0.0445, wR_2 = 0.1070.

5: *$[TBA]_6\{[C_2H_5C(CH_2O)_3]CrMo_6O_{18}[(OCH_2)_3CNH_2]\}_2 \cdot 3DMF$.* $C_{125}H_{275}Cr_2Mo_{12}N_{11}O_{51}$, M_r = 4003.83, orthorhombic, space group

DOI: 10.1021/ic502622k
Inorg. Chem. 2015, 54, 2551−2559

Scheme 1. Stepwise Modification Process for the Synthesis of Asymmetrically Triol-Functionalized Anderson Clusters

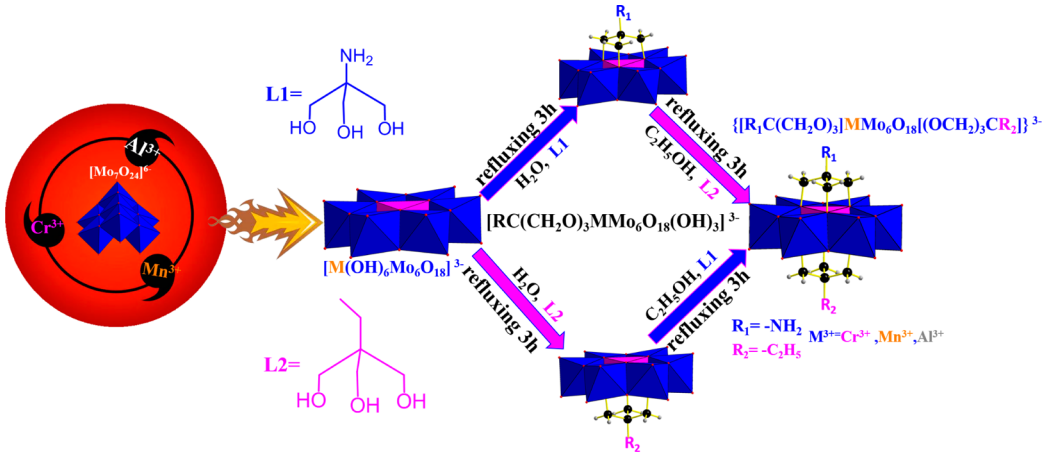

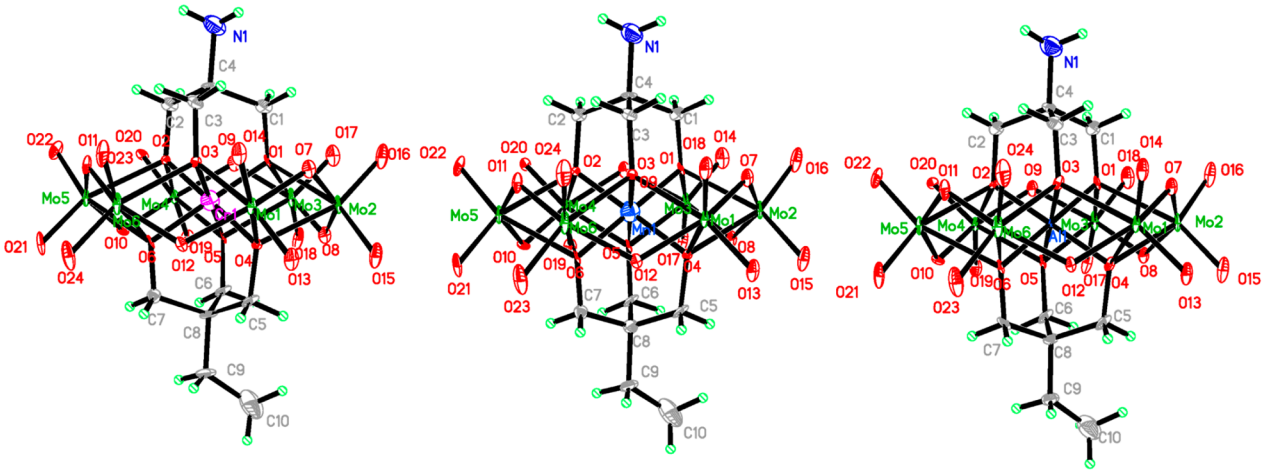

Figure 1. ORTEP drawings of the cluster anions of the asymmetrically triol-functionalized hybrids: compounds **5** (left), **6** (middle), and **7** (right). Thermal ellipsoids are drawn at the 30% probability level.

$P2_12_12_1$, a = 13.5976(2), b = 49.5568(7), c = 25.3420(4) Å, $\alpha = \gamma = \beta$ = 90°, V = 17076.8(5) Å^3, Z = 8, T = 293(2) K, 31 086 reflections measured, R_1(final) = 0.0586, wR_2 = 0.1173.

6: *[TBA]$_6${[$C_2H_5C(CH_2O)_3$]$MnMo_6O_{18}$[$(OCH_2)_3CNH_2$]}$_2$·4DMF*. $C_{128}H_{292}Mn_2Mo_{12}N_{12}O_{52}$, M_r = 4092.89, orthorhombic, space group $P2_12_12_1$, a = 13.7969(1), b = 49.1579(8), c = 25.2437(5) Å, $\alpha = \gamma = \beta$ = 90°, V = 17120.9(6) Å^3, Z = 8, T = 293(2) K, 30 886 reflections measured, R_1(final) = 0.0513, wR_2 = 0.1090.

7: *[TBA]$_6${[$C_2H_5C(CH_2O)_3$]$AlMo_6O_{18}$[$(OCH_2)_3CNH_2$]}$_2$·3DMF*. $C_{125}H_{275}Al_2Mo_{12}N_{11}O_{51}$, M_r = 3953.80, orthorhombic, space group $P2_12_12_1$, a = 13.6974(3), b = 49.3570(6), c = 25.1423(3) Å, $\alpha = \gamma = \beta$ = 90°, V = 16997.8(5) Å^3, Z = 8, T = 293(2) K, 30 256 reflections measured, R_1(final) = 0.0498, wR_2 = 0.1018.

DFT Stimulated NMR ^{1}H Spectrum Calculations. All of the calculations presented herein were carried out with the Gaussian09 program package. The structures of each stationary point were fully optimized using the B3LYP method[28] in combination with the LANL2DZ basis set for molybdate, chromium, and aluminum atoms and the 6-31+G(d) basis set for other main group elements. Configurations were optimized before Mulliken charge analysis and stimulated NMR ^{1}H spectrum calculation.The calculation was completed on the Explorer 100 cluster system of the Tsinghua National Laboratory for Information Science and Technology.

RESULTS AND DISCUSSION

Synthesis Strategy. As shown in Scheme 1, the single-sided triol-functionalized precursors $[TBA]_3[RC(CH_2O)_3MMo_6O_{18}(OH)_3]$ (compound **1**: M = Cr^{3+}, R = NH_2; compound **2**: M = Cr^{3+}, R = C_2H_5; compound **3**: M = Mn^{3+}, R = NH_2; compound **4**: M = Al^{3+}, R = C_2H_5) were synthesized first. Then, the as-prepared single-sided triol-functionalized precursors reacted with another type of triol ligand in hot ethanol for ca. 3 h to afford the asymmetric double-sided triol-functionalized Anderson derivatives, $[TBA]_3\{[R_1C(CH_2O)_3]MMo_6O_{18}[(OCH_2)_3CR_2]\}$ (R_1 = NH_2, R_2 = C_2H_5; compound **5**: M = Cr^{3+}; compound **6**: M = Mn^{3+}; compound **7**: M = Al^{3+}) in ca. 80% yields. Due to the stepwise synthetical protocol, the possibility of symmetric byproduct formation has been totally ruled out. However, in order to make ESI-MS monitoring detectable, two kinds of triol ligands with different molecular weights were selected: $(HOCH_2)_3CNH_2$ (L1) and $(HOCH_2)_3CC_2H_5$ (L2). Moreover, compound **5** can be effectively obtained either from compound **1** or compound **2** in excellent yields; this implies that the order in which the triol ligands are anchored on the parent Anderson cluster in aqueous solution does not affect the generation of the final asymmetric hybrid products. Compared to the reported one-pot reaction,[22,23] this two-step protocol operates easily on the bench, saves time, is more controllable, and provides target-oriented products with high purity and good yield.

DOI: 10.1021/ic502622k
Inorg. Chem. 2015, 54, 2551−2559

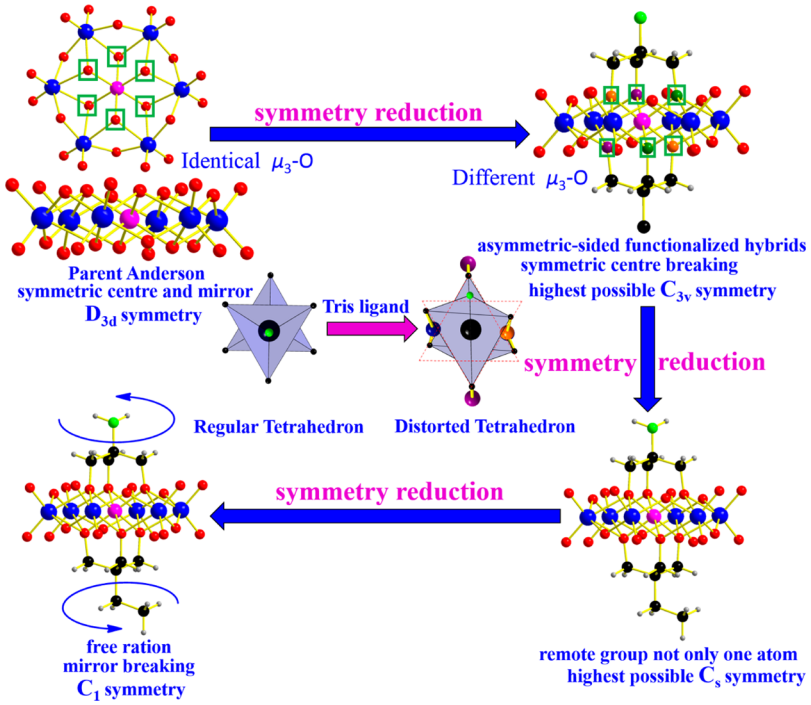

Figure 2. Generation of intrinsic chirality through stepwise double-sided asymmetric triol functionalization.

Structure Description. The molecular structures of compounds **1**−**7** have been confirmed definitively by single-crystal X-ray diffraction. ORTEP drawings of the cluster anions of double-sided asymmetric triol-funtionalized hybrids **5**−**7** and single-sided triol-funtionalized hybrids **1**−**4** are shown in Figures 1 and S2, respectively. The geometry of the asymmetric hybrid polyanions was based on a common Anderson structure: Six edge-sharing MoO_6 octahedrals were arranged around a central MO_6 unit and six μ_3-OH groups are replaced by two types of triol ligands.[29] Compared with the length of C-(μ_3-O) in previously reported symmetrically triol-funtionalized hybrids, which have a narrow range from 1.434 to 1.466 Å, these asymmetrical products have a wider range, from 1.397 to 1.471 Å.

It should be noted that asymmetrically triol-funtionalized hybrid compounds **5**−**7** all crystallized in orthorhombic chiral space group $P2_12_12_1$. This suggests that these compounds are perhaps chiral and also indicated that, through stepwise asymmetric triol functionalization, achiral precursors may be transferred into chiral products and spontaneous resolution occurs.

After careful examination of the molecular structures of these compounds, we discovered that double-sided asymmetrically triol-functionalized hybrids were intrinsically chiral indeed. As shown in Figure 2, the origin of their chirality can be understood by the following symmetry reduction demonstration: The parent Anderson cluster was achiral due to its D_{3d} symmetry; it contains a symmetric center and three mirrors. However, its D_{3d} symmetry will be reduced to the highest possible C_{3v} symmetry when two types of triol ligands are anchored on each side of the parent Anderson cluster, thus removing the symmetric center. Yet, it is an extreme situation that these two triol ligands also have C_{3v} symmetry and the three substituted μ_3-O groups on each side remain equivalent after covalent modification.

In most cases, both assumptions are not met; hence, the highest possible symmetry will be reduced to C_s symmetry if these two triol ligands have a common mirror while they are anchored on the parent Anderson cluster and if this mirror coincides with one of the three mirrors in the parent Anderson cluster. However, due to free rotation on both of the remote moieties of these two triol ligands, it is impossible that both triol ligands could simultaneously have a stable coplanar conformation that coincides with three of the mirrors in the parent Anderson cluster. This indicates that it is very difficult to force both triol ligands to stay in such a special position simultaneously to maintain mirror symmetry. In other words, the final symmetry of the double-sided asymmetric triol-functionalized Anderson clusters was C_1. Hence, these hybrids are chiral; this is in agreement with the fact that compounds **5**−**7** all crystallized in a chiral space group, as confirmed by single-crystal X-ray diffractions studies.

The packing mode of compound **5** in a 2 × 2 × 2 super cell unit was projected in the 010 direction of the crystal plane (*b* axis). To demonstrate the packing mode clearly, it can be assumed that in the middle point of the line that linked two central heteroatoms of two cluster units nearby there was a hypothetical axis in which the cluster units pack one by one in a zigzag manner with the same remote moiety orientated in the same direction while each cluster unit is offset from the center of the hypothetical axis with a distance of 7.14 nm, forming a 2_1 helix along this hypothetical axis projected on the *c* axis and forming a 1D infinite chain substructure-based layer-by-layer structure.

Regarding the intrinsic chirality of the asymmetric hybrids, it was actually a chiral helical chain possessing a 2_1 helical axis. The solvent-accessible voids in the crystals formed chiral channels that were moderate in diameter, 3.7 nm, which is about 24% of the super cell's volume (Figure 3).

Spontaneous Resolution from a Mixed Solvent System. Because the double-sided asymmetric triol-function-

DOI: 10.1021/ic502622k
Inorg. Chem. 2015, 54, 2551−2559

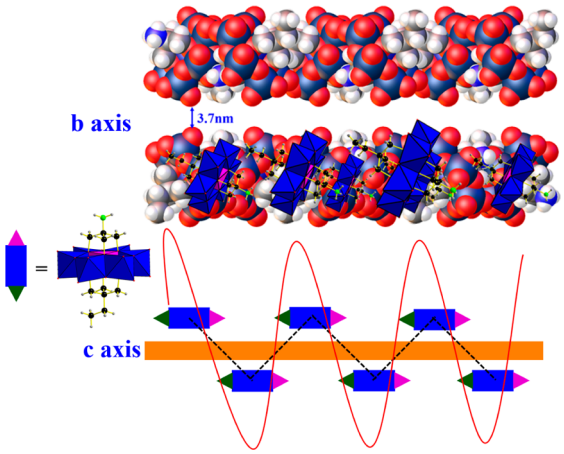

Figure 3. Packing mode of compound **5** (ball and stick and space filling) along the *b* and *c* directions.

alized hybrids were intrinsically chiral, their spontaneous resolution may occur under suitable solvent conditions. In our previous work,[24b] we discovered that the DMF/MeCN mixed solvent system worked very well for the spontaneous resolution of single-sided triol-functionalized hybrids. On the basis of this, we supposed that this DMF/MeCN mixed solvent system may also work for these asymmetric triol-functionalized hybrids because of the structural similarity of these asymmetric triol-functionalized hybrids and their single-sided triol-functionalized precursors. Hence, we applied pure and mixed organic solvents of DMF/MeCN with different ratios for the spontaneous resolution of these asymmetric hybrids (see Table S1 in the Supporting Information). In a 65:35 DMF/MeCN mixed solvent, the spontaneous resolution of compounds **5**−**7** occurs. This is not rare and is an ideal starting point for the generation of chiral species.

Spectra Characterization. *IR Spectra Characterization.* The IR spectra obtained in the solid-state was analyzed in detail. IR spectra of compounds **5**−**7** (see Figure S5) were very similar to each other and were in agreement with those of typical Anderson-type structures. Herein, for compound **5**, the characteristic peaks at 937, 921, and 902 cm^{-1} were assigned to the vibrations of terminal Mo═O units, and those at 740 and 662 cm^{-1} belonged to the vibrations of the Mo−O−Mo groups. The only detectable difference between the asymmetrically triol-functionalized hybrids and the single-sided triol-functionalized precursors was the vibration peak of the C−O bonds, which demonstrated grafting of the triol onto the surface of POM. In compound **1**, only one C−O vibration band was detected at 1050 cm^{-1}, whereas in compound **5**, the peak of the C−O bonds split into two peaks at 1080 and 1042 cm^{-1}. This was attributed to the triols asymmetrically ligating on the parent Anderson cluster.

The structures of compounds **1**−**7** have also been investigated by EA, ESI-MS, and ^{1}H and ^{13}C NMR (Figures S3−S6).

UV−Vis Spectra Characterization. To confirm the absorption bands located in both the ultraviolet and visible regions, UV spectra were recorded before obtaining circular dichroism spectra. Compared with the LMCT absorption band of the parent Anderson cluster, $[Cr(OH)_6Mo_6O_{18}]^{3-}$, located around 238 nm, which primarily corresponded to a ligand-centered μ_3-OH π to metal-centered Mo^{6+} t_{2g}* charge transfer transition (LMCT), the LMCT bands of compounds **1** and **5** show a slight hypsochromic shift to 224 and 211 nm, respectively (ε_{LMCT} = 4.66 × 10^5 and 4.83 × 10^5 $L{\cdot}mol^{-1}{\cdot}cm^{-1}$ for compounds **1** and **5**, respectively). This was due to the increase in the crystal field splitting energy. The hypsochromic shift in compound **5** is more obvious than that in compound **1** because μ_3-OCH_2 is a stronger field ligand than μ_3-OH. Compared with the parent Anderson cluster, both sides of μ_3-OH were substituted by μ_3-OCH_2 in compound **5**, whereas only one side was in compound **1**. The d−d transition absorption band of $[Cr(OH)_6Mo_6O_{18}]^{3-}$ located around 540 nm was assigned to the metal-centered lowest-energy electronic transition from HOMO t_{2g}* to LUMO e_g* of Cr^{3+}. A similar hypsochromic shift phenomenon was observed in compound **1** at 534 nm and compound **5** at 526 nm (ε_{d-d} = 5.66 × 10^2 and 5.91 × 10^2 $L{\cdot}mol^{-1}{\cdot}cm^{-1}$ for compounds **1** and **5**, respectively). It should be noted that the hypsochromic shift phenomenon appearing at the d−d transition band was assigned to the reduction of charge density in μ_3-O when triol ligands were anchored on it. A similar hypsochromic shift was observed in compounds **6** and **7**. The LMCT bands were located at 212 and 241 nm for compounds **6** and **7**, respectively, and d−d transition absorption existed only in compound **6**, which was located at 460 nm (see Figure S6). It should be noted that the locations of the d−d transition absorption of compounds **5**−**7** that led to color formation was consistent with the color that these compounds possessed: pink, orange, and colorless for compounds **5**−**7**, respectively (see Figure S1).

CD Spectra Characterization. To further examine the stable chiroptical activity of these asymmetric hybrids in the solid state, their circular dichroism (CD) spectra were measured as follows: A sufficient amount of single crystals of the asymmetric hybrids was picked from the crystallization solution randomly and immediately used in a KBr pellet CD test. It should be noted that aggregations of enantiopure crystals have to be sorted manually to obtain either positive or negative signals randomly by this method. However, it is feasible to pick each enantiomer to conduct CD if one picks enough crystals on the basis of probability. It should be noted that such chirality was stable only in the solid state. Stable chirality in solution was a more vital issue because it could afford potential applications of these hybrid materials in chiral oxidation catalysis and chiral separation. The chiral stability of the solution of compound **7** was also investigated. Similar signal was detected in the liquid state, but, unfortunately, the lifetime was not long enough. The signal was gradually attenuated to zero response within 1.5 h after testing. Free rotation of C−N and C−C bonds in solution results in fast racemization because the free rotation energy barriers of C−N and C−C bonds are not very high at room temperature. However, the chiral stability of these enantiopure asymmetric hybrids in solution has been further imporved compared with that of the enantiopure single-sided precursors that we reported previously as a result of both sides of the Anderson custer being modified by triol ligands.[24b]

In the solid-sate CD spectra of compound **7**, two Cotton effects were observed. The positive and negative signals afforded were approximately the mirror image of each other (Figure 4). The Cotton effects in the ultraviolet band around 200 and 212 nm that were characteristic of the absorption were in accordance with the corresponding absorption band in the UV spectrum (Figure S6). No Cotton effect signal was detected in the visible band, which was reasonable since the color of compound **7**'s crystal was colorness and a d−d transition did not exist for the Al ion.

DOI: 10.1021/ic502622k
Inorg. Chem. 2015, 54, 2551−2559

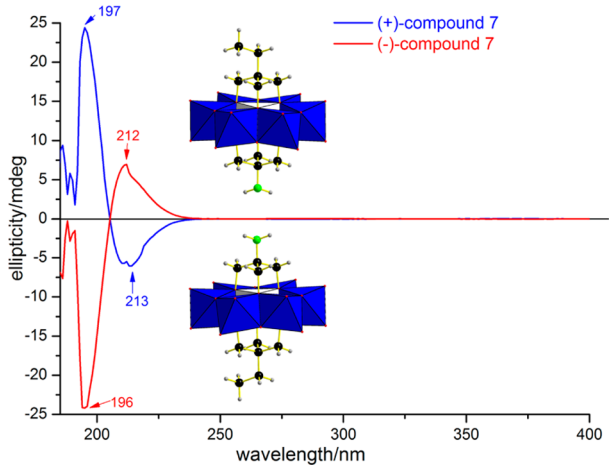

Figure 4. Solid-state CD spectra of enantiopure crystal grains of compound **7**.

However, only one Cotton effect in the ultraviolet region was observed in compounds **5** and **6** (Figure S7). The absence of a Cotton effect signal in the visible region was confusing, as the crystals of these two compounds were colored. Then, we found that, compared with the ε_{LMCT} of the Cotton effect signal located in the ultraviolet band, the ε_{d-d} of the Cotton effect signal in the visible band was a thousandth of the ε_{LMCT} value, which was assigned to the metal-centered lowest-energy electronic transition from HOMO t_{2g}* to LUMO e_g*, resulting in color formation. Therefore, it was too weak to detect both of them simultaneously. Considering that only a single crystal was picked to record the CD spectra, the concentration was not high enough to detect this Cotton effect signal in the visible band. However, considering the case of compound **7**, the results indicated that the chirality of these asymmetrically triol-functionalized hybrids was maintained in the solid state. Moreover, information found in the absolute chemical configuration in the CIF files revelaed that these asymmetric hybrids were "ad", which means that the absolute configuration can be determined by the Flack parameter. The Flack[30a] and Hooft[30b] parameter values all approached zero (see Table S2 in the Supporting Information). This means that spontaneous resolution occurs instead of racemization and that the absolute configuration was definitely and correctly determined

Feasibility Investigation of the Stepwise Protocol. The feasibility of the stepwise protocol for the asymmetric triol functionalization of a parent Anderson cluster was also investigated by DFT calculations (Figure 5). The sequence energy E_{UB3LYB} from high to low was as follows: parent Anderson cluster > single-sided triol-functionalized derivatives > asymmetrically triol-functionalized derivatives. This clearly indicated that the stepwise protocol was definitely feasible from a thermodynamics standpoint since entropy increased using this process when two types of triol ligands were anchored on the parent Anderson cluster sequentially. From dynamics, the traditional triol-functionalized Anderson derivative synthesis route (synthesis route 2 in Figure 6) involved complex POM

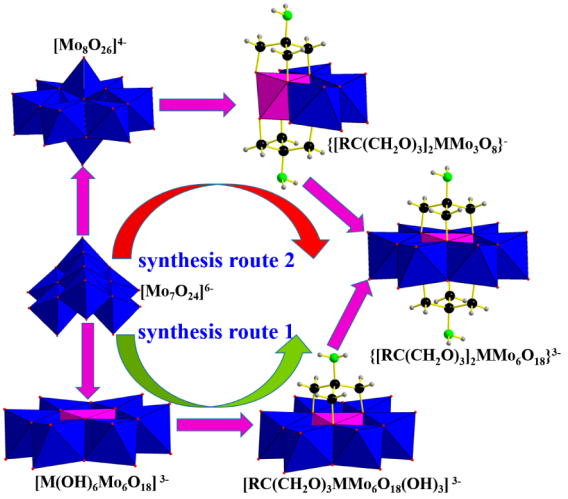

Figure 6. Comparison of traditional and stepwise routes for the synthesis of Anderson triol-functionalized derivatives.

reconstruction and underwent a higher transition state. The stepwise protocol (synthesis route 1 in Figure 6) simplified this by using precise and controllable μ_3-OH reactive sites in the parent Anderson cluster, which greatly reduces the activation energy. Therefore, such a protocol was also a dynamics preferred process. Additionally, from the standpoint of reactivity, the stepwise protocol allowed us to apply a flexible POMs–linker strategy to design and functionalize this organic–inorganic hybrid because it can conveniently stay in

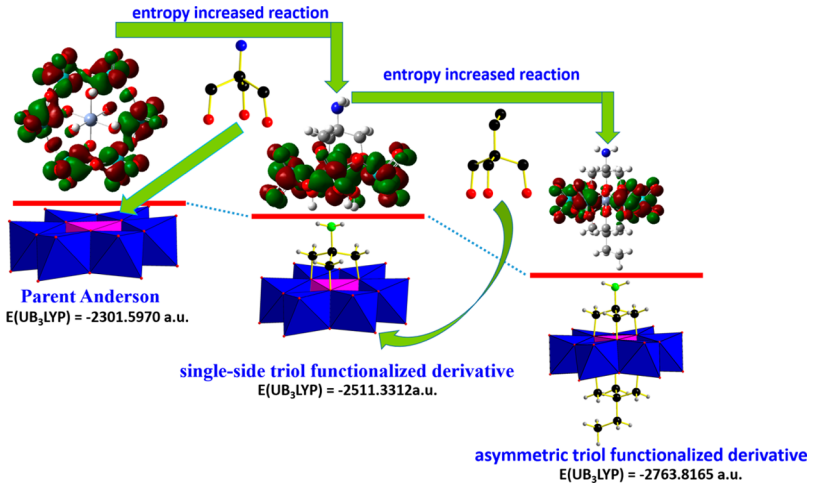

Figure 5. Energy E_{UB3LYB} of the reactants and products in the stepwise asymmetric triol-functionalization process.

DOI: 10.1021/ic502622k
Inorg. Chem. 2015, 54, 2551–2559

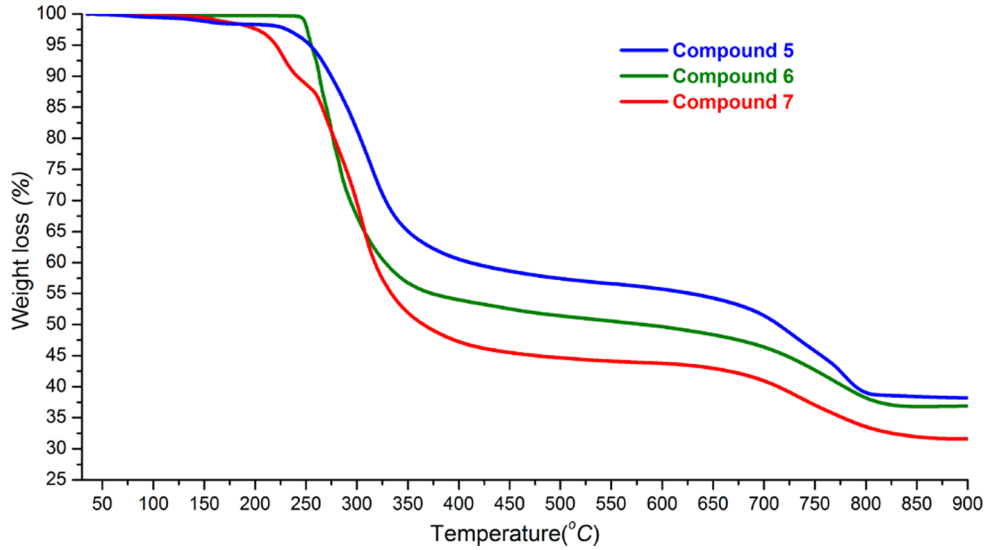

Figure 7. Thermal stability of asymmetrically triol-functionalized hybrids compounds **5**–**7**.

a single-sided triol-functionalized precursor intermediate state. The hybrids can be regarded as bifunctionalized monomers that possess remote reactive moieties, i.e., triol ligand, and remaining μ_3-OH reactive sites for further modification.

Thermal Stability. Thermal gravimetric analysis (TGA) measurements were used to test the weight loss and to examine the thermal stability of these asymmetrically triol-functionalized hybrids, compounds **5**–**7**. Their thermal stabilities were slightly different since the central heteroatom was different in each. Cr–Anderson compound **5** and Mn–Anderson compound **6** showed good thermal stability up to 250 °C, whereas Al–Anderson compound **7** was somewhat unstable and started to decompose at 180 °C. This indicated that the species of the central heteroatom has a significant effect on the stability of these asymmetric hybrids. Cr–Anderson and Mn–Anderson asymmetric hybrids were more stable than Al–Anderson asymmetric hybrids. The weight loss processes of these compounds were also quite different. Cr–Anderson compound **5** displayed three weight loss steps; the first step at 250–350 °C was the expulsion three TBA counterions with a 38.48% weight loss. This was in excellent agreement with the calculated value of 38.44%. The second step at 350–740 °C was the complete decomposition of the organic triol moiety and the decomposition of the cluster into MoO_3 and CrO_3 with a 10.63% weight loss. The last step, starting at 740 °C, was the partial sublimation of MoO_3 with 8.34% weight loss. For Mn–Anderson compound **6**, there was only one wide-ranging weight loss step, including the complete decomposition of three TBA counterions, organic triol moiety, and the cluster into MoO_3 and MnO_2 followed by the partial sublimation of MoO_3 with a total 60.11% weight loss at temperature 250–810 °C. For Al–Anderson compound **7**, there were also three steps; however, the order of the decomposition was quite different that that of compound **5**. The first step was the complete decomposition of the organic triol moiety at 180–250 °C with an 8.24% weight loss. Then the second step was the expulsion three TBA counterions at 250–360 °C with a 38.93% weight loss. The last step was the decomposition of the cluster into MoO_3 and Al_2O_3 followed by the partial sublimation of MoO_3 with a 21.11% weight loss at 350–850 °C. The different decomposition order between compounds **5** and **7** indicated another important fact, namely, that the triol ligand was more stable when it was anchored on a Cr–Anderson cluster than an Al–Anderson cluster (Figure 7).

CONCLUSIONS

In summary, using a convenient two-step esterification reaction, three novel asymmetrically triol-functionalized Anderson cluster derivatives were efficiently synthesized in high purity and good yields, which was carried out easily on the bench without further separation and purification. The direct triol functionalization of a parent Anderson cluster should be a flexible strategy that can be applied to tune and functionalize a POMs cluster and that could be extended to other types of Anderson clusters. TGA measurements indicated that the species of the central heteroatom has a significant effect on the stability of these asymmetric hybrids. As confirmed by single-crystal X-ray diffraction and solid-state CD spectra, the asymmetric hybrids are chiral. They could be used as potential synthons for developing POM-based chiral hybrid materials. For example, hybrids with a reactive amino group are of great importance because they can serve as perfect synthons for the investigation of chiral self-assembly[31] via a state-of-the-art postmodification synthetic strategy[32] (Figure 8). The feasibility of such a protocol was also investigated by DFT calculations.

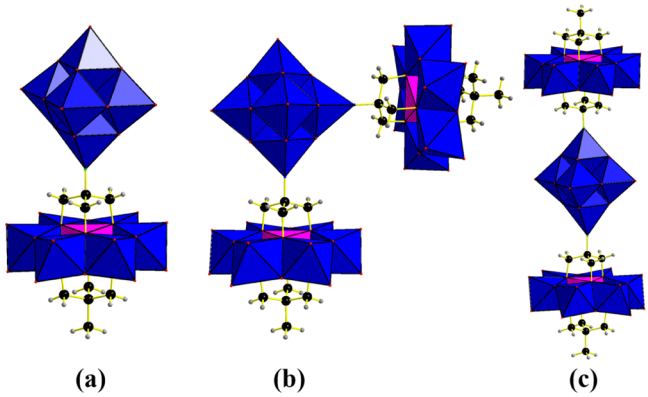

Figure 8. Related investigation of the chiral self-assembly of asymmetrically triol-functionalized hybrids via imidoylization modification.

DOI: 10.1021/ic502622k
Inorg. Chem. 2015, 54, 2551–2559

Such organic−inorganic hybrid materials possess a layer-by-layer structure, forming solvent-accessible nanoscale chiral channels via a 1D infinite helical chain substructure. Such POMs-based hybrid materials may have potential applications in chiral catalysis and chiral separation, and related work is under way in our laboratory.

■ ASSOCIATED CONTENT

Supporting Information

Related crystallographic and DFT calculations details as well as NMR, IR, UV, ESI-MS, and CD spectra studies. This material is available free of charge via the Internet at http://pubs.acs.org. CCDC 977519, 977523, and 1020979−1020983 contain the supplementary crystallographic data for this article. These data can be obtained free of charge from The Cambridge Crystallographic Data Centre via www.ccdc.cam.ac.uk/data_request/cif.

■ AUTHOR INFORMATION

Corresponding Authors

*(Jianhui Luo) E-mail: luojh@petrochina.com.cn.
*(Jin Zhang) E-mail: jinjin_eva@mail.tsinghua.edu.cn.
*(Yongge Wei) E-mail: yonggewei@mail.tsinghua.edu.cn.

Notes

The authors declare no competing financial interest.

■ ACKNOWLEDGMENTS

We are grateful for financial support from the National Natural Science Foundation of China (NSFC nos. 21225103, 21471087, 21301105, and 21221062), Beijing Natural Science Foundation (no. 2144051), China National Petroleum & Gas Corporation Science and Technology Development Project "Nano Intelligent Chemical Flooding Agent" (2014A-1001), Tsinghua University Initiative Foundation Research Program (no. 20131089204), THSJZ, and the open project of the Key Laboratory of Polyoxometalate Science of the Ministry of Education of China.

■ REFERENCES

(1) (a) Zuo, T. M.; Beavers, C. M.; Duchamp, J. C.; Campbell, A.; Dorn, H. C.; Olmstead, M. M.; Balch, A. L. *J. Am. Chem. Soc.* **2007**, *129*, 2035−2043. (b) Zhao, D.; Timmons, D. J.; Yuan, D. Q.; Zhou, H. C. *Acc. Chem. Res.* **2011**, *44*, 123−133.

(2) (a) Lin, F.; Peng, H. Y.; Chen, J. X.; Chik, D. T. W.; Cai, Z. W.; Wong, K. M. C.; Yam, V. W. W.; Wong, H. N. C. *J. Am. Chem. Soc.* **2010**, *132*, 16383−16392. (b) Zaleski, C. M.; Depperman, E. C.; Kampf, J. W.; Kirk, M. L.; Pecoraro, V. L. *Inorg. Chem.* **2006**, *45*, 10022−10024.

(3) (a) Sanchez-Valencia, J. R.; Dienel, T.; Groning, O.; Shorubalko, I.; Mueller, A.; Jansen, M.; Amsharov, K.; Ruffieux, P.; Fasel, R. *Nature* **2014**, *512*, 61−64. (b) Friedfeld, M. R.; Shevlin, M.; Hoyt, J. M.; Krska, S. W.; Tudge, M. T.; Chirik, P. J. *Science* **2013**, *342*, 1076−1080. (c) Singh, G.; Chan, H.; Baskin, A.; Gelman, E.; Repnin, N.; Kral, P.; Klajn, R. *Science* **2014**, *345*, 1149−1153.

(4) (a) Li, S. S.; Northrop, B. H.; Yuan, Q. H.; Wan, L. J.; Stang, P. J. *Acc. Chem. Res.* **2009**, *42*, 249−259. (b) Coric, I.; List, B. *Nature* **2012**, *483*, 315−319. (c) Barrett, K. T.; Metrano, A. J.; Rablen, P. R.; Miller, S. J. *Nature* **2014**, *509*, 71−75. (d) Hyster, T. K.; Knorr, L.; Ward, T. R.; Rovis, T. *Science* **2012**, *338*, 500−503. (e) Du, J. N.; Skubi, K. L.; Schultz, D. M.; Yoon, T. P. *Science* **2014**, *344*, 392−396.

(5) (a) Pope, M. T.; Müller, A. *Angew. Chem., Int. Ed. Engl.* **1991**, *30*, 34−48. (b) Rhule, J. T.; Hill, C. L.; Judd, D. A. *Chem. Rev.* **1998**, *98*, 327−357.

(6) (a) Weinstock, I. A.; Barbuzzi, E. M. G.; Wemple, M. W.; Cowan, J. J.; Reiner, R. S.; Sonnen, D. M.; Heintz, R. A.; Bond, J. S.; Hill, C. L. *Nature* **2001**, *414*, 191−195. (b) Douglas, T.; Young, M. *Nature* **1998**, *393*, 152−155.

(7) Fang, X. K.; Anderson, T. M.; Hill, C. L. *Angew. Chem., Int. Ed.* **2005**, *44*, 3540−3544.

(8) Carraro, M.; Sartorel, A.; Scorrano, G.; Maccato, C.; Dickman, M. H.; Kortz, U.; Bonchio, M. *Angew. Chem., Int. Ed.* **2008**, *47*, 7275−7279.

(9) Zang, H. Y.; Miras, H. N.; Yan, J.; Long, D. L.; Cronin, L. *J. Am. Chem. Soc.* **2012**, *134*, 11376−11379.

(10) An, H. Y.; Wang, E. B.; Xiao, D. R.; Li, Y. G.; Su, Z. M.; Xu, L. *Angew. Chem., Int. Ed.* **2006**, *45*, 904−908.

(11) (a) Bareyt, S.; Piligkos, S.; Hasenknopf, B.; Gouzerh, P.; Lacote, E.; Thorimbert, S.; Malacria, M. *J. Am. Chem. Soc.* **2005**, *127*, 6788−6794. (b) Micoine, K.; Hasenknopf, B.; Thorimbert, S.; Lacote, E.; Malacria, M. *Angew. Chem., Int. Ed.* **2009**, *48*, 3466−3468.

(12) (a) Zhang, J.; Hao, J.; Wei, Y.; Xiao, F.; Yin, P.; Wang, L. *J. Am. Chem. Soc.* **2010**, *132*, 14−15. (b) Xiao, F. P.; Hao, J.; Zhang, J.; Lv, C. L.; Yin, P. C.; Wang, L. S.; Wei, Y. G. *J. Am. Chem. Soc.* **2010**, *132*, 5956−5957.

(13) Soghomonian, V.; Chen, Q.; Haushalter, R. C.; Zubieta, J.; Oconnor, C. J. *Science* **1993**, *259*, 1596−1599.

(14) (a) Proust, A.; Matt, B.; Villanneau, R.; Guillemot, G.; Gouzerh, P.; Izzet, G. *Chem. Soc. Rev.* **2012**, *41*, 7605−7622. (b) Banerjee, A.; Bassil, B. S.; Roschenthaler, G. V.; Kortz, U. *Chem. Soc. Rev.* **2012**, *41*, 7590−7604.

(15) (a) Li, D.; Song, J.; Yin, P. C.; Simotwo, S.; Bassler, A. J.; Aung, Y. Y.; Roberts, J. E.; Hardcastle, K. I.; Hill, C. L.; Liu, T. B. *J. Am. Chem. Soc.* **2011**, *133*, 14010−14016. (b) Yin, P. C.; Wu, P. F.; Xiao, Z. C.; Li, D.; Bitterlich, E.; Zhang, J.; Cheng, P.; Vezenov, D. V.; Liu, T. B.; Wei, Y. G. *Angew. Chem., Int. Ed.* **2011**, *50*, 2521−2525.

(16) (a) Zeng, H. D.; Newkome, G. R.; Hill, C. L. *Angew. Chem., Int. Ed.* **2000**, *39*, 1772−1774. (b) Pradeep, C. P.; Long, D. L.; Newton, G. N.; Song, Y. F.; Cronin, L. *Angew. Chem., Int. Ed.* **2008**, *47*, 4388−4391.

(17) (a) Hasenknopf, B.; Delmont, R.; Herson, P.; Gouzerh, P. *Eur. J. Inorg. Chem.* **2002**, 1081−1087. (b) Marcoux, P. R.; Hasenknopf, B.; Vaissermann, J.; Gouzerh, P. *Eur. J. Inorg. Chem.* **2003**, 2406−2412.

(18) (a) Song, Y. F.; Long, D. L.; Cronin, L. *Angew. Chem., Int. Ed.* **2007**, *46*, 3900−3904. (b) Zhang, J.; Song, Y.-F.; Cronin, L.; Liu, T. *J. Am. Chem. Soc.* **2008**, *130*, 14408−14409. (c) Song, Y.-F.; McMillan, N.; Long, D.-L.; Kane, S.; Malm, J.; Riehle, M. O.; Pradeep, C. P.; Gadegaard, N.; Cronin, L. *J. Am. Chem. Soc.* **2009**, *131*, 1340−1341. (d) Rosnes, M. H.; Musumeci, C.; Pradeep, C. P.; Mathieson, J. S.; Long, D.-L.; Song, Y.-F.; Pignataro, B.; Cogdell, R.; Cronin, L. *J. Am. Chem. Soc.* **2010**, *132*, 15490−15492. (e) Yvon, C.; Surman, A. J.; Hutin, M.; Alex, J.; Smith, B. O.; Long, D. L.; Cronin, L. *Angew. Chem., Int. Ed.* **2014**, *53*, 3336−3341.

(19) (a) Favette, S.; Hasenknopf, B.; Vaissermann, J.; Gouzerh, P.; Roux, C. *Chem. Commun.* **2003**, 2664−2665. (b) Santoni, M. P.; Pal, A. K.; Hanan, G. S.; Proust, A.; Hasenknopf, B. *Inorg. Chem.* **2011**, *50*, 6737−6745.

(20) (a) Yan, Y.; Wang, H. B.; Li, B.; Hou, G. F.; Yin, Z. D.; Wu, L. X.; Yam, V. W. W. *Angew. Chem., Int. Ed.* **2010**, *49*, 9233−9236. (b) Yue, L.; Ai, H.; Yang, Y.; Lu, W. J.; Wu, L. X. *Chem. Commun.* **2013**, *49*, 9770−9772.

(21) Wilson, E. F.; Miras, H. N.; Rosnes, M. H.; Cronin, L. *Angew. Chem., Int. Ed.* **2011**, *50*, 3720−3724.

(22) Song, Y. F.; Long, D.-L.; Kelly, S. E.; Cronin, L. *Inorg. Chem.* **2008**, *47*, 9137−9139.

(23) Yvon, C.; Macdonell, A.; Buchwald, S.; Surman, A. J.; Follet, N.; Alex, J.; Long, D. L.; Cronin, L. *Chem. Sci.* **2013**, *4*, 3810−3817.

(24) (a) Wu, P. F.; Yin, P. C.; Zhang, J.; Hao, J.; Xiao, Z. C.; Wei, Y. G. *Chem.—Eur. J.* **2011**, *17*, 12002−12005. (b) Zhang, J. W.; Zhao, Z. L.; Zhang, J.; She, S.; Huang, Y. C.; Wei, Y. G. *Dalton Trans* **2014**, *43*, 17296−17302.

(25) Nomiya, K.; Takahashi, T.; Shirai, T.; Miwa, M. *Polyhedron* **1987**, *6*, 213−218.

(26) Sheldrick, G. M. *Acta. Crystallogr., Sect. A* **2008**, *64*, 112−122.

DOI: 10.1021/ic502622k
Inorg. Chem. 2015, 54, 2551−2559

(27) Dolomanov, O. V.; Bourhis, L. J.; Gildea, R. J.; Howard, J. A. K.; Puschmann, H. *J. Appl. Crystallogr.* **2009**, *42*, 339−341.
(28) (a) Becke, A. D. J *Chem. Phys.* **1993**, *98*, 5648−5652. (b) Lee, C. T.; Yang, W. T.; Parr, R. G. *Phys. Rev. B* **1988**, *37*, 785−789.
(29) Zhang, J. W.; Huang, Y. C.; Zhang, J.; She, S.; Hao, J.; Wei, Y. G. *Dalton Trans* **2014**, *43*, 2722−2725.
(30) (a) Flack, H. D.; Bernardinelli, G. *Acta Crystallogr., Sect. A* **1999**, *55*, 908−915. (b) Hooft, R. W. W.; Straver, L. H.; Spek, A. L. *J. Appl. Crystallogr.* **2008**, *41*, 96−103.
(31) Yin, P. C.; Zhang, J.; Li, T.; Zuo, X. B.; Hao, J.; Warner, A. M.; Chattopadhyay, S.; Shibata, T.; Wei, Y. G.; Liu, T. B. *J. Am. Chem. Soc.* **2013**, *135*, 4529−4536.
(32) (a) Zhang, J.; Xiao, F. P.; Hao, J.; Wei, Y. G. *Dalton Trans.* **2012**, *41*, 3599−3615. (b) Zhang, J. W.; Hao, J.; Khan, R. N. N.; Zhang, J.; Wei, Y. G. *Eur. J. Inorg. Chem.* **2013**, 1664−1671.

DOI: 10.1021/ic502622k
Inorg. Chem. 2015, 54, 2551−2559